

Repulsive exciton-exciton interaction in quantum dots

S. Rodt,* R. Heitz, A. Schliwa, R. L. Sellin, F. Guffarth, and D. Bimberg

Institut für Festkörperphysik, Technische Universität Berlin, Hardenbergstrasse 36, 10623 Berlin, Germany

(Received 14 April 2003; published 30 July 2003)

Biexcitons localized in single InAs/GaAs quantum dots (QD's) are investigated by cathodoluminescence, demonstrating an anticorrelation of the biexciton binding energy and the exciton transition energy. The binding energy decreases with increasing transition energy changing its sign at about 1.24 eV. The “binding” to “antibinding” transition is attributed to three-dimensional confinement, quenching correlation, and exchange and causing local charge separation. Model calculations of the biexciton in truncated InAs/GaAs QD's demonstrate the observed trend to result from the decreasing number of localized excited states with decreasing QD size. The interaction with resonant states in the wetting layer is found to be negligible.

DOI: 10.1103/PhysRevB.68.035331

PACS number(s): 78.67.Hc, 71.45.Gm, 73.21.La, 78.60.Hk

For few-particle states localized in semiconductor quantum dots (QD's) the interrelation of the Coulomb interaction and confinement in determining the electronic properties is not clear, yet. A detailed understanding of such few-particle states is of interest both from a fundamental physics point of view as well as for applications, possibly providing a pathway to utilize the structural properties of self-organized QD's as design parameters.¹ In particular the exciton-biexciton system is crucial for single-photon emitters^{2,3} and entangled qubit registers⁴ in quantum cryptography and quantum computing, respectively. Here, the renormalization of the exciton transition energy by a spectator exciton—i.e., the biexciton binding energy—is important, allowing one to address the exciton and biexciton selectively.

In semiconductor structures with spatial dispersion the biexciton is the bound state of two excitons and the binding energy is defined as the energy gain with respect to two spatially separated excitons. The biexciton binding energy is much smaller than the exciton binding energy and, thus, can in first order be described by correlation and exchange of the two neutral excitons. Confinement in one or more directions reduces the exciton Bohr radius and thus increases the biexciton binding energy.^{5–7} For self-organized In(Ga)As/GaAs QD's a large spread of binding energies was reported, ranging from sporadic negative values^{2,3,8} up to ~ 5 meV (see e.g. Refs. 9 and 10). Remarkably, all the QD's emit in the same spectral region, suggesting a pronounced impact of the detailed structural properties. However, no correlation to structural or electronic properties of the investigated QD's was attempted, yet.

In self-organized QD's the Coulomb interaction of the four localized fermions of a biexciton is dominated by the kinetic confinement energy. Though in principle the notion of two interacting excitons is no longer appropriate, it is still useful in describing experiments and shall be maintained in the following. The properties of few-particle states obviously depend on the structural properties of the QD's, which might vary in a wide range. Remarkably, calculations predict that confinement can result in a negative biexciton binding energy,^{11–13} indicating a repulsive Coulomb interaction between the two localized “excitons.” In this case the biexciton might be dubbed “antibinding” although the four-particle state is still stable due to the confinement potential.

Here we present a first systematic investigation of the biexciton binding energy in self-organized InAs/GaAs QD's, demonstrating an anticorrelation between the binding energy and the exciton transition energy. Comparing a large number of single QD's for a given sample in cathodoluminescence (CL) experiments a transition from positive to negative biexciton binding energy with decreasing QD size is observed. Model calculations accounting for the details of the confinement potential resulting from the inhomogeneous strain, band mixing, and the piezoelectric potential show that the biexciton binding energy is determined by the confinement-dependent interplay of direct Coulomb interaction and correlation and exchange.

The investigated samples were grown by metalorganic chemical vapor deposition on semi-insulating GaAs (001) substrates. First, 300 nm GaAs followed by 50 nm AlGaAs and 100 nm GaAs were grown as buffer. Next 1.7 monolayer (ML) of InAs were deposited at 485 °C followed by a growth interruption,¹⁴ resulting in the formation of QD's in the Stranski-Krastanow mode. Finally, the QD's were capped with 50 nm GaAs followed by 20 nm AlGaAs and 20 nm GaAs. Transmission electron micrographs show a QD sheet density of $5 \times 10^{10} \text{ cm}^{-2}$ and suggest flat, truncated pyramidal QD's with base lengths around 13 nm. Cross-sectional scanning tunneling images support the formation of truncated InAs/GaAs QD's under the used growth conditions.¹⁵

The optical properties of the QD ensemble provide further insight into the structural properties. Photoluminescence was investigated with a tungsten lamp dispersed by a 0.27-m double-grating monochromator as tunable excitation source and a Ge diode in conjunction with a 0.3-m double-grating monochromator for detection. Figure 1(a) shows a photoluminescence spectrum at 7 K of a typical sample. The QD peak centered at about 1.2 eV shows a modulation of the intensity, which is typical for samples grown under similar conditions. Detailed optical and growth studies, which are beyond the scope of the present paper, show that the modulation reflects a multimodal distribution of the ground-state transition energy in the QD ensemble, which can be traced to ML steps of the QD height.¹⁶ Model calculations show that the discrete energy jumps are in good agreement with InAs/GaAs QD's having a flat, truncated pyramidal shape with well-defined upper and lower interfaces.

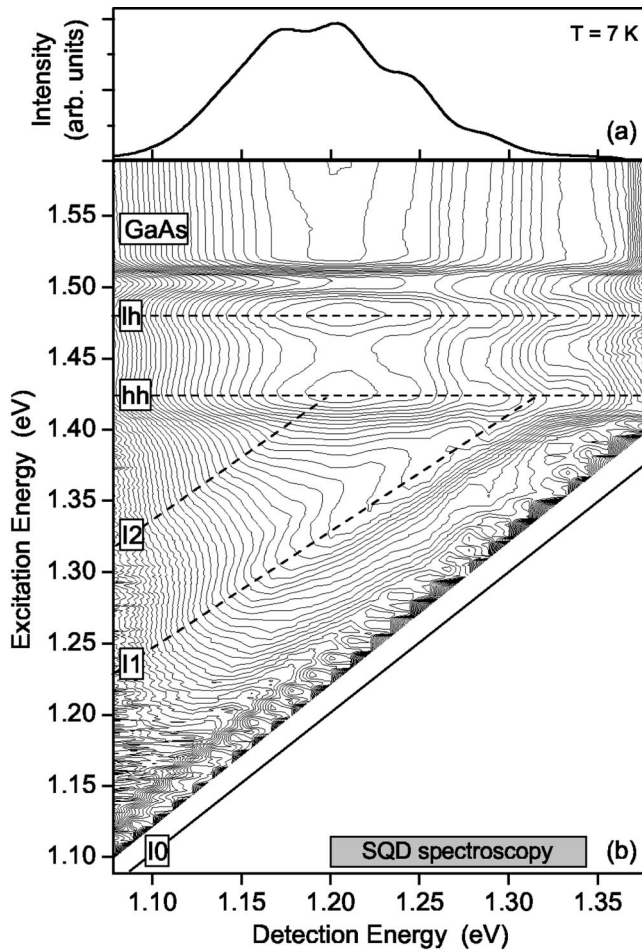


FIG. 1. Photoluminescence spectrum (a) and photoluminescence excitation contour plot (b). The centers of the ground-state transition (I0) and of the first (I1) and second (I2) excited state transitions are marked by the skew lines. Horizontal lines denote the heavy-hole (hh) and light-hole (lh) resonances of the wetting layer. Single QD's (SQD's) were probed in the energy range marked by the gray bar.

As will be argued below the renormalization of the biexciton transition depends critically on the spectrum of excited exciton states, which can be revealed by photoluminescence excitation (PLE) spectroscopy.¹⁷ Figure 1(b) depicts a contour plot of the photoluminescence intensity as a function of the detection and excitation energies on a logarithmic scale. In the upper part of the plot, absorption in the GaAs matrix and in the wetting layer leads to intense nonselective luminescence. The heavy hole (hh) resonance of the wetting layer at 1.42 eV marks the onset of the continuum that limits localization in the QD's. At lower detection energies absorption of the first (I1) and second (I2) excited exciton transitions are resolved. The large splittings of ~ 140 meV between the ground state (I0) and I1 and ~ 100 meV between I1 and I2 indicate strong quantization, which we attribute to the small size and high indium content of the investigated QD's. Obviously, the number of bound excited exciton states depends on the ground state energy—i.e., the size of the QD's [Fig. 1(b)]: With increasing (decreasing) ground-state energy (QD size) the excited states are eventu-

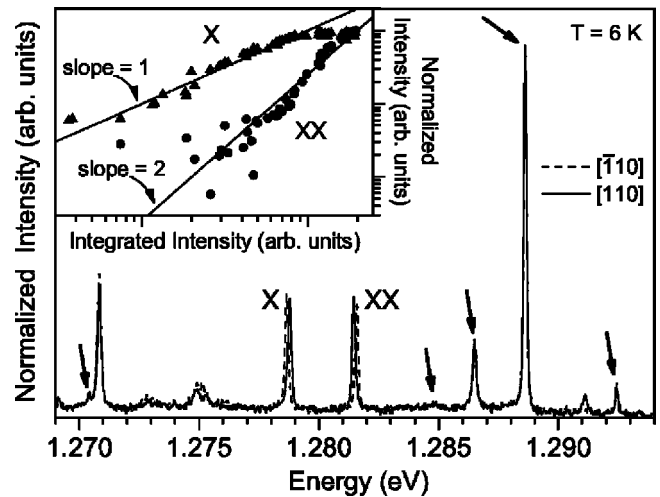


FIG. 2. Polarized CL spectra. The emissions marked by X, XX, and arrows belong to a single QD. Inset: intensities of the X and XX recombination as a function of the integrated intensity. The lines indicate slopes of 1 and 2, respectively.

ally pushed into the wetting layer turning into resonant states.

In order to investigate biexcitons localized in the InAs/GaAs QD's it is necessary to probe single QD's. Therefore CL measurements were performed in a JEOL JSM 840 scanning electron microscope at an acceleration voltage of 7 kV with the sample mounted on the cold finger of a variable-temperature He-flow cryostat. Luminescence was dispersed by a 0.3-m monochromator with a 1200 grooves/mm grating and detected with a Si-CCD detector, providing a spectral resolution better than $140 \mu\text{eV}$. The Si detector allows to probe QD's with a ground state transition energy in the energy range marked by the gray bar in Fig. 1(b). For reproducible measurements on particular QD's, Au shadow masks with circular apertures of ~ 100 nm diameter were used, limiting simultaneous optical access to four QD's on average.

A representative CL spectrum, as shown in Fig. 2, consists of a rather large number of sharp lines, which might originate from various few-particle complexes in different QD's. It is, however, possible to identify the exciton and biexciton emissions of a single QD in a three-step process. First, the spectrum of a single QD is identified by the omnipresent spectral jitter of the transition energies (not shown here).¹⁸ The statistical variation of the local electric field, and therefore the variation of the spectral shift caused by the quantum-confined Stark effect, is distinct for each QD. Typically, about seven emission lines are observed for a single QD (marked by X, XX, and arrows in Fig. 2). Second, the exciton/biexciton emissions are cross-polarized doublets of identical splitting but reversed polarization with respect to [110] (lines X and XX in Fig. 2). The observed splittings between $60 \mu\text{eV}$ and $134 \mu\text{eV}$ are attributed to the fine structure splitting of the bright exciton state caused by the reduced symmetry of the confinement potential resulting from the piezoelectric potential¹⁹ and a possible lateral elongation of the QD's.²⁰ The lack of a measurable fine structure of the other emissions suggests recombination of charged

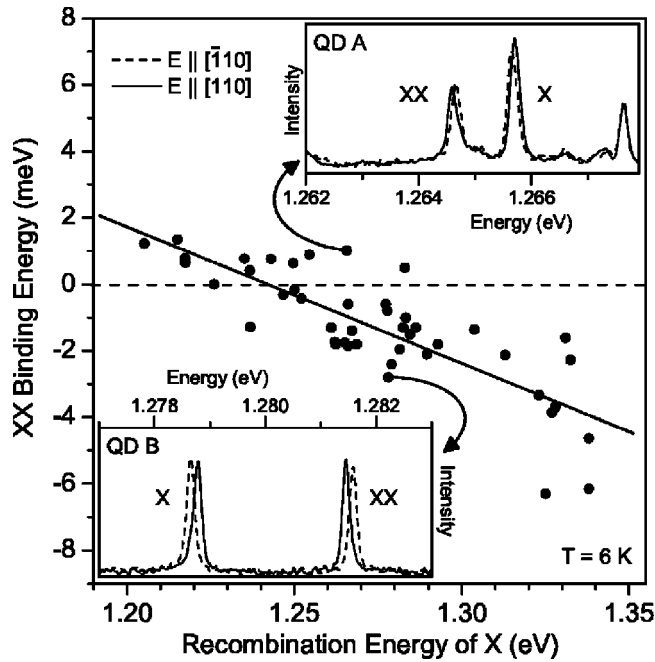


FIG. 3. Biexciton binding energy vs exciton recombination energy for 46 QD's. The line is a linear fit to the data as guide to the eye. Insets: polarized emission spectra of two QD's demonstrating a binding (QD A) and an antibinding (QD B) biexciton complex, respectively.

exciton complexes, for which either the electron or hole spin is paired off, quenching the exchange interaction. Charged exciton complexes have been investigated in detail recently.^{9,10} Finally, the exciton and biexciton emissions are identified by the characteristic excitation density dependences as depicted in the inset of Fig. 2. The effective excitation density was varied scanning the electron beam across the aperture and using the integrated intensity as reference. The exciton appears first with a slope of ~ 1 whereas the biexciton intensity depends quadratically on the excitation density.²¹

In the following we will concentrate on the biexciton binding energy. The insets of Fig. 3 depict polarized emission spectra of two different QD's with similar exciton recombination energy. The biexciton appears once at lower (QD A) and once at higher (QD B) energy than the exciton. The respective energy shifts of 1 meV and -3 meV demonstrate the wide variation of the biexciton binding energy in the investigated sample, allowing even for a sign reversal. Obviously, the Coulomb interaction of the two localized excitons can be either attractive or repulsive—i.e., either binding or antibinding. The main part of Fig. 3 compiles the biexciton binding energy in 46 different QD's as a function of the exciton transition energy. The binding energy varies between 1.3 meV and -6.3 meV and, in spite of some scatter, exhibits a clear trend: The binding energy decreases with increasing exciton recombination energy. The line is a linear fit as guide to the eye, showing the transition from a binding to an antibinding biexciton complex at an exciton recombination energy of ~ 1.24 eV.

The scatter of the biexciton binding energy for a given

exciton transition energy highlights the importance of the actual confining potential—i.e., of structural properties like shape and composition. Note that different QD's might have the same exciton transition energy. A pronounced impact of the QD shape on the biexciton binding energy was recently predicted for truncated pyramidal InAs/GaAs QD's.^{13,22} Whereas an antibinding biexciton is expected for pyramidal QD's, it becomes binding for truncated ones with a small height to base length ratio. As outlined above, structural and optical data indicate a flat truncated shape for the InAs/GaAs QD's investigated here, implying a binding biexciton complex as indeed observed for the larger QD's emitting below ~ 1.24 eV. The calculations²² fail, however, to explain the antibinding biexciton complex in the smaller QD's emitting around 1.3 eV.

The biexciton binding energy results from the Coulomb interaction of the four fermions (two electrons and two holes) localized in the confinement potential of the QD. The binding energy is defined as the energy difference between two independent excitons and the biexciton. For self-organized InAs/GaAs QD's, the kinetic confinement energy dominates the Coulomb interaction¹⁷ which limits the ability of the wave functions to adapt in the few-particle states. This is particularly important for strained QD's for which the confinement leads to local charge separation due to the inhomogeneous strain and the piezoelectric quadrupole potential.¹⁹ Though the exciton binding energy is always positive, the repulsive electron-electron and hole-hole interactions overcompensate the attractive electron-hole interaction in the four particle complex, providing for a repulsive direct Coulomb contribution to the biexciton binding energy. The repulsive direct Coulomb energy can be of the order of 10 meV in pyramidal QD's but strongly decreases truncating the QD's.^{12,13,22} The binding contribution to the biexciton binding energy results from correlation and exchange, which in total might lead to a binding biexciton state. Indeed, the binding biexciton complexes observed for QD's with transition energies smaller than 1.24 eV are in good agreement with the predictions for flat truncated InAs/GaAs QD's.²²

The observed decrease of the binding energy with increasing transition energy is attributed to a decreasing impact of correlation and exchange. On the one hand, the larger quantization in smaller QD's reduces the contribution of excited exciton states to the biexciton ground state.²³ On the other hand, the finite barrier potential in the InAs/GaAs system limits the number of localized exciton states in the QD's.^{11,19} As demonstrated by the PLE results in Fig. 1(b) with increasing exciton transition energy the excited exciton states are successively pushed into the wetting layer, becoming resonant states. Indeed, the smallest QD's probed in the single-QD experiments (Fig. 3) have no excited states at all, whereas for the largest ones even 12 is observed. The decreasing number of localized excited states in the smaller QD's reduces the impact of exchange and correlation, being in qualitative agreement with the observed trend as well as the antibinding biexciton complexes in the smaller QD's.

For the purpose of calculating the biexciton binding energy in self-organized QD's, we start with single-particle wave functions calculated within an eight-band $\mathbf{k}\cdot\mathbf{p}$ frame-

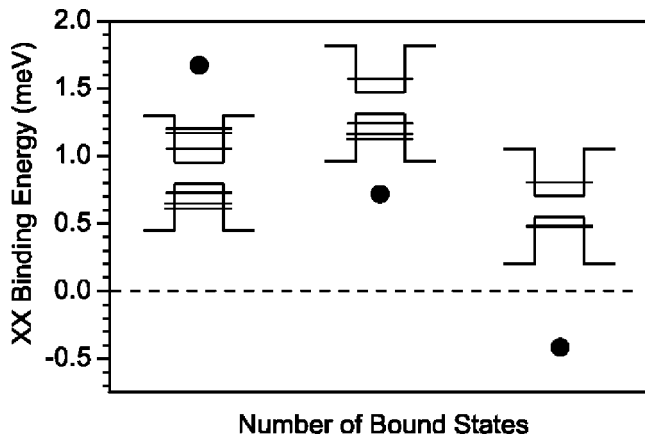


FIG. 4. Calculated biexciton binding energies for a truncated InAs/GaAs QD taking into account different numbers of bound states as depicted by the QD schemes.

work including strain, spin-orbit interaction, band mixing, interband coupling, and piezoelectricity.¹⁹ The single-particle wave functions carry the structural information of the QD's and are subsequently used to calculate few-particle states in a configuration interaction scheme to account for the Coulomb interaction including correlation and exchange. Both exciton and biexciton complexes are calculated directly from the single-particle wave functions rather than successively as implied by the notion of a biexciton. Figure 4 shows the biexciton binding energy predicted for a truncated pyramidal InAs/GaAs QD with a height of 5 ML and a base length of 13 nm as a function of the size of the configuration room. Taking into account the lowest three spin-degenerated electron and hole states leads to a positive binding energy of about 1.7 meV in good agreement with the experimental results for the largest probed QD's (see Fig. 3). Restricting the configuration room and, finally, taking into account only the ground states causes a transition to an antibinding biexciton in qualitative agreement with the results for the smaller

QD's. The calculations support that the observed transition from a binding to an antibinding biexciton complex with decreasing QD size results from the delocalization of the excited states due to the finite barrier height. We conclude that the Coulomb interaction with delocalized states in the wetting layer is negligible for the biexciton binding energy.

Finally, the observed biexciton binding energies are significantly lower than most reported values.^{9,10,24} We suggest that the composition of the QD's makes the difference. The large substate splitting (>100 meV) in the present samples indicates a high indium content and quenches the impact of correlation and exchange. An increasing gallium admixture reduces the substate splitting and increases the number of excited states²⁵ and, thus, increases the binding contribution of correlation and exchange. Indeed, InGaAs QD's have been studied in most reported single-QD experiments.

In conclusion, the biexciton binding energy in flat, truncated InAs/GaAs QD's was investigated, demonstrating a systematic dependence on the QD size. With decreasing QD size the biexciton complex changes from binding to antibinding. The occurrence of an antibinding biexciton is attributed to the impact of the confining potential, which generates a repulsive effect of the direct Coulomb interaction, and the decreasing number of localized excited states with decreasing QD size, which quenches the impact of correlation and exchange. In particular the latter effect accounts for the observed systematic decrease of the biexciton binding energy. The results demonstrate the biexciton binding energy to be a sensitive measure for the structural properties of self-organized QD's as well as the impact of the Coulomb interaction with delocalized states to be negligible.

We thank N. Zakharov and P. Werner for transmission electron microscopy. The electronic-structure calculations were performed on the Cray T3E computer of the Konrad-Zuse-Zentrum Berlin. Parts of this work were supported by Deutsche Forschungsgemeinschaft in the framework of SFB 296 and by INTAS Project No. 99-00928.

*Electronic address: srodt@physik.TU-Berlin.DE

¹D. Bimberg, *et al.*, *Quantum Dot Heterostructures* (Wiley, Chichester, 1999).

²R.M. Thompson, R.M. Stevenson, A.J. Shields, I. Farrer, C.J. Lobo, D.A. Ritchie, M.L. Leadbeater, and M. Pepper, *Phys. Rev. B* **64**, 201302 (2001).

³E. Moreau, I. Robert, L. Manin, V. Thierry-Mieg, J.M. Gérard, and I. Abram, *Phys. Rev. Lett.* **87**, 183601 (2001).

⁴G. Chen, T.H. Stievater, E.T. Batteh, X. Li, D.G. Steel, D. Gammon, D.S. Katzer, D. Park, and L.J. Sham, *Phys. Rev. Lett.* **88**, 117901 (2002).

⁵G.W. 't Hooft, W.A.J.A. van der Poel, L.W. Molenkamp, and C.T. Foxon, *Phys. Rev. B* **35**, 8281 (1987).

⁶P. Borri, W. Langbein, J.M. Hvam, and F. Martelli, *Phys. Rev. B* **60**, 4505 (1999).

⁷T. Baars, W. Braun, M. Bayer, and A. Forchel, *Phys. Rev. B* **58**, R1750 (1998).

⁸L. Landin, M.-E. Pistol, C. Pryor, M. Persson, L. Samuelson, and

M. Miller, *Phys. Rev. B* **60**, 16 640 (1999).

⁹J.J. Finley, P.W. Fry, A.D. Ashmore, A. Lemaître, A.I. Tartakovskii, R. Oulton, D.J. Mowbray, M.S. Skolnick, M. Hopkinson, P.D. Buckle, and P.A. Maksym, *Phys. Rev. B* **63**, 161305 (2001).

¹⁰M. Baier, F. Findeis, A. Zrenner, M. Bichler, and G. Abstreiter, *Phys. Rev. B* **64**, 195326 (2001).

¹¹Ph. Lelong, O. Heller, and G. Bastard, *Solid-State Electron.* **42**, 1251 (1998).

¹²O. Stier, in *Nano-Optoelectronics*, edited by M. Grundmann (Springer-Verlag, Berlin, 2002), p. 167.

¹³O. Stier, A. Schliwa, R. Heitz, M. Grundmann, and D. Bimberg, *Phys. Status Solidi B* **224**, 115 (2001).

¹⁴F. Heinrichsdorff, A. Krost, D. Bimberg, A.O. Kosogov, and P. Werner, *Appl. Surf. Sci.* **123/124**, 725 (1998).

¹⁵H. Eisele, O. Flebbe, T. Kalka, F. Heinrichsdorff, A. Krost, D. Bimberg, and M. Dähne-Prietsch, *Phys. Status Solidi B* **215**, 865 (1999).

¹⁶R. Heitz, F. Guffarth, K. Pötschke, A. Schliwa, and D. Bimberg (unpublished).

- ¹⁷R. Heitz, O. Stier, I. Mukhametzhano, A. Madhukar, and D. Bimberg, *Phys. Rev. B* **62**, 11 017 (2000).
- ¹⁸V. Türck, S. Rodt, O. Stier, R. Heitz, R. Engelhardt, U.W. Pohl, D. Bimberg, and R. Steingrüber, *Phys. Rev. B* **61**, 9944 (2000).
- ¹⁹O. Stier, M. Grundmann, and D. Bimberg, *Phys. Rev. B* **59**, 5688 (1999).
- ²⁰V.D. Kulakovskii, G. Bacher, R. Weigand, T. Kümmell, A. Forchel, E. Borovitskaya, K. Leonardi, and D. Hommel, *Phys. Rev. Lett.* **82**, 1780 (1999).
- ²¹M. Grundmann and D. Bimberg, *Phys. Rev. B* **55**, 9740 (1997).
- ²²O. Stier, R. Heitz, A. Schliwa, and D. Bimberg, *Phys. Status Solidi A* **190**, 477 (2002).
- ²³S. Schmitt-Rink, D.A.B. Miller, and D.S. Chemla, *Phys. Rev. B* **35**, 8113 (1987).
- ²⁴M. Bayer, O. Stern, P. Hawrylak, S. Fafard, and A. Forchel, *Nature (London)* **405**, 923 (2000).
- ²⁵F. Heinrichsdorff, M. Grundmann, O. Stier, A. Krost, and D. Bimberg, *J. Cryst. Growth* **195**, 540 (1998).